ANL/CHM/CP-98671

For submission to the 11th Symposium on Separation Science and Technology for Energy Applications, Gatlinburg, TN, October 17-21, 1999.

Aggregation of Dialkyl-Substituted Diphosphonic Acids and its Effect on Metal Ions Extraction*

R. CHIARIZIA[1], R. E. BARRANS, Jr. and J. R. FERRARO
Chemistry Division, Argonne National Laboratory, Argonne, IL 60439, USA

A. W. HERLINGER and D. R. McALISTER
Department of Chemistry, Loyola University Chicago, Chicago, IL 60626, USA

ABSTRACT

Solvent extraction reagents containing the diphosphonic acid group exhibit an extraordinary affinity for tri-, tetra- and hexavalent actinides. Their use has been considered for actinide separation and pre-concentration procedures. Solvent extraction data obtained with P,P'-di(2-ethylhexyl) methane-, ethane- and butanediphosphonic acids exhibit features that are difficult to explain without knowledge of the aggregation state of the extractants. Information about the aggregation of the dialkyl-substituted diphosphonic acids in aromatic diluents has been obtained using the complementary techniques of vapor pressure osmometry (VPO), small angle neutron scattering (SANS), infrared spectroscopy and molecular mechanics. The results from these techniques provide an understanding of the aggregation behavior of these extractants that is fully compatible with the solvent extraction data. The most important results and their relevance to solvent extraction are reviewed in this paper.

[1]To whom correspondence should be addressed.

*The work at ANL was performed under the auspices of the Office of Basic Energy Sciences, Division of Chemical Sciences, U.S. Department of Energy, under contract W-31-109-ENG-38.

DISCLAIMER

INTRODUCTION

Aqueous soluble diphosphonic acids are powerful complexing agents for a wide variety of metal ions, especially actinides and lanthanides (1,2). The chelating ion exchange resin Diphonix® contains a geminally substituted diphosphonic acid ligand chemically bonded to a styrene-based polymeric matrix. Because of its extraordinarily strong affinity for actinide ions and for iron(III), the resin has found application in procedures for actinide separations and in hydrometallurgical processes where efficient separation of Fe(III) from other transition metals is required (3).

P,P'-di(alkyl) alkyldiphosphonic acids are the solvent extraction equivalent of the Diphonix resin. A general formula for some recently developed dialkyl-substituted diphosphonic acid solvent extraction reagents is shown in Structure **I**:

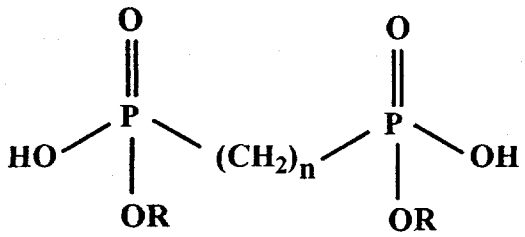

Structure **I**

where R is the 2-ethylhexyl group and n is one, two or four, for P,P'-di(2-ethylhexyl) methane- (H_2DEH[MDP]), ethane- (H_2DEH[EDP]), and butane- (H_2DEH[BuDP]) diphosphonic acids, respectively. The recently developed extraction chromatographic resin Dipex® is a noteworthy example of a practical application of H_2DEH[MDP] in actinide separation procedures (4).

It is well established that acidic organophosphorus extractants strongly aggregate in non-polar diluents (5,6). Monoprotic acids usually dimerize to form an $\mathbf{R_2^2(8)}$ ring, analogous to that formed in the familiar dimerization of carboxylic acids. $\mathbf{R_2^2(8)}$, in the Etter hydrogen bond assembly classification (7), denotes an 8-membered ring structure containing two hydrogen bond donors and two hydrogen bond acceptors. Hydrogen bonding in organophosphorus acid dimers, however, is known to be stronger than in carboxylic acid dimers (8,9). The aggregation behavior of diprotic acids is more complicated. When two monomers hydrogen bond to form a dimeric species containing one $\mathbf{R_2^2(8)}$ ring, the resulting aggregate has additional -OH groups that can serve as sites for further aggregation (10). This explains why di(2-ethylhexyl) phosphoric acid, HDEHP, is dimeric in benzene (6,11), while the diprotic acid mono(2-ethylhexyl) phosphoric acid, H_2MEHP, can have an aggregation number as high as 12 in the same diluent (11,12).

Since HDEHP and H_2MEHP can be regarded as monofunctional analogues of the diphosphonic acids shown in Structure I, the question arises whether the aggregation

behavior of H_2DEH[MDP], H_2DEH[EDP] and H_2DEH[BuDP] is similar to that of a dibasic acid or if aggregation is limited to the formation of dimers like a monobasic acid.

Knowledge of the aggregation state of an extractant is important not only from a basic structural point of view, but it is also vital for understanding metal extraction chemistry, especially, the interpretation of the slope values of extractant dependencies. In solvent extraction systems characterized by extensive extractant aggregation, extractant dependencies are generally unity and independent of the type of metal ion extracted. This type of behavior has been reported for the extraction of actinides and lanthanides by H_2MEHP in aromatic diluents (10,12,13). With highly aggregated extractants, such as H_2MEHP, metal ions are buried within the extractant aggregate and held in place by forces analogous to those in solid ion exchange resins (10). Similar results have been reported for other highly aggregated extractants, e.g., quaternary alkylammonium salts (14) and dinonylnaphthalene sulfonic acid in non-depolymerizing diluents (15). These examples illustrate the effect that the aggregation state of the extractant molecule can have on the metal extraction chemistry.

The aggregation behavior of H_2DEH[MDP], H_2DEH[EDP] and H_2DEH[BuDP] in aromatic diluents has been investigated by infrared spectroscopy, vapor pressure osmometry (VPO), molecular mechanics methods and small angle neutron scattering (SANS). These complementary techniques have provided valuable insights into the unique metal solvent extraction data exhibited by these compounds. The objective of the present work is to summarize the results of our recent aggregation studies and illustrate how these results provide an understanding of the metal solvent extraction chemistry.

EXPERIMENTAL

Materials

The preparation, purification and properties of H_2DEH[MDP], H_2DEH[EDP] and H_2DEH[BuDP], as well as the radioisotopes and other reagents used in this work have been reported previously (16-18).

Techniques

The distribution ratio measurements were performed as reported in references 16-18. The details of the VPO and IR measurements can be found in references 18-23. The SANS measurements on deuterated toluene solutions of H_2DEH[MDP], H_2DEH[EDP] and H_2DEH[BuDP] and their metal complexes were made using the time-of-flight small-angle neutron diffractometers SAD and SAND at the Intense Pulsed Neutron Source (IPNS) at Argonne National Laboratory. The characteristics of the diffractometers, the data treatment and the equations used to calculate the weight-average aggregation number, **n**, of the aggregates have been reported in earlier studies (24-26). The details of the molecular mechanics calculations on H_2DEH[MDP] can be found in (23).

RESULTS AND DISCUSSION

Solvent extraction data

Distribution data have been obtained for the extraction of alkaline earth cations (Ca^{+2}, Sr^{+2}, Ba^{+2} and Ra^{+2}), Fe(III), and representative tri-, tetra- and hexavalent actinide ions (Am(III), Th(IV) and U(VI)) by o-xylene solutions of H_2DEH[MDP], H_2DEH[EDP] and H_2DEH[BuDP]. For each metal ion-extractant system, acid and extractant dependencies have been determined. A complete account of the extraction data can be found in references 16-18. Some representative data, however, will be presented here.

Figures 1 summarizes the extractant dependencies measured for the extraction of Am(III) by H_2DEH[MDP], H_2DEH[EDP] and H_2DEH[BuDP] in o-xylene. Similar results were obtained for alkaline earth cations and U(VI) (16-18). The data of Figure 1 show that the slope values of the extractant dependencies measured for H_2DEH[MDP] and H_2DEH[BuDP] are equal to 2, while those measured for H_2DEH[EDP] are equal to 1. Based on the arguments presented earlier, this behavior led us to suspect that H_2DEH[MDP] and H_2DEH[BuDP] form small aggregates in o-xylene, while H_2DEH[EDP] may form much larger aggregates. To obtain a quantitative estimate of the extractant aggregation, however, different types of measurements were needed.

Infrared spectroscopy

Infrared spectra of 0.15 M toluene solutions of H_2DEH[MDP], H_2DEH[EDP] and H_2DEH[BuDP] are shown in Figure 2. A complete discussion of these spectra and their changes upon metal extraction has been given in references 18-23. In this presentation, only spectral features that are directly related to extractant aggregation will be discussed.

There are no absorption bands in the spectra shown in Figure 2 that can be attributed to free hydroxyl groups. Three broad bands of medium intensity, characteristic of the P(O)(OH) group of an alkyl phosphonic acid, appear at relatively low frequencies at about 2700, 2300 and 1700 cm^{-1}. This behavior is characteristic of O-H groups that are strongly involved in hydrogen bonding to phosphoryl oxygen atoms (11,12). These three bands disappear upon metal salt formation as expected.

Some of the strongest absorption bands in the spectra occur in the 950-1250 cm^{-1} region. The band at ~1200 cm^{-1} is of particular interest. This band has been assigned as a phosphoryl absorption by comparison with the spectra of related organophosphorus acids (27,28). The frequency of this band is considerably lower than that reported for the corresponding tetra-ethyl esters due to strong hydrogen bonding with the P-OH group (29). These spectral features, characteristic of strongly intermolecularly hydrogen bonded systems, clearly indicate that H_2DEH[MDP], H_2DEH[EDP] and H_2DEH[BuDP] exist in solutions as aggregates. Strong hydrogen bonding is, in fact, the key to the stability of the

aggregates. No quantitative information on the type of aggregates, i.e., dimers vs. higher aggregates, however, is provided by the infrared spectra.

A striking feature of the H_2DEH[MDP] spectrum is the P=O band splitting. For H_2DEH[EDP] and H_2DEH[BuDP] a single broad P=O stretching band is observed. The appearance of two bands in the P=O stretching region of the spectrum of H_2DEH[MDP] initially led to the hypothesis that two different types of hydrogen bonds, i.e., intra- and intermolecular, were present in the aggregate. The appearance of a single phosphoryl band in the spectra of H_2DEH[EDP] and H_2DEH[BuDP] implied that all the hydrogen bonds in the aggregate are equivalent.

IR spectra of toluene solutions of H_2DEH[MDP], H_2DEH[EDP] and H_2DEH[BuDP] after metal extraction from aqueous solutions in some cases showed water absorption bands at ~3400 and ~1660 cm^{-1}. This indicates that with some metal ions, water as well as the metal ions are extracted by the diphosphonic acids. Although no quantitative study of water extraction was performed, the water absorption bands were particularly strong in the extraction of alkaline earth cations and Eu(III) by H_2DEH[EDP]. H_2DEH[EDP] is unique in its ability to extract water. In fact, even solutions of H_2DEH[EDP] pre-equilibrated with aqueous nitric acid in the absence of metal ions exhibit characteristic water absorption bands. Co-extraction of water is generally observed when the extractant forms large aggregates in the organic phase that behave like reverse micelles (30,31).

Osmometric measurements

Vapor pressure osmometry (VPO) measurements on toluene solutions of H_2DEH[MDP], H_2DEH[EDP] and H_2DEH[BuDP] were used to determine aggregation numbers for these extractants in a non-polar diluent (18-20). Some typical results are compared in Figure 3 with data for the monomeric standard bibenzyl. To a first approximation, in the concentration range investigated, the VPO plots are linear. Thus, the aggregation number (**n**) of an extractant can be obtained simply from the ratio of the slope of the standard to that of the extractant. The data in Figure 3 clearly indicate that H_2DEH[MDP] forms dimeric species, while H_2DEH[EDP] and H_2DEH[BuDP] form hexameric and trimeric aggregates, respectively.

Complementary VPO measurements were run on solutions of the extractants after loading the organic phase with selected metal ions through solvent extraction. The data revealed that in several cases, at high metal concentrations in the organic phase, the metal-extractant complexes were highly aggregated. This was particularly evident for the Fe(III)-H_2DEH[MDP] and the Fe(III)-H_2DEH[BuDP] systems, for which average aggregation numbers as high as ~33 and ~18, respectively, were obtained. With H_2DEH[EDP], the average aggregation number remained essentially unchanged after extraction of metal ions at high concentration. This implies that in many cases the

hexameric aggregation of the extractant is not disrupted by the extraction of metal ions. This result reaffirms the unique solvent extraction behavior of H_2DEH[EDP].

The highly aggregated state of H_2DEH[EDP], which is not disrupted by metal extraction, explains the extractant dependencies reported in Figure 1. Assuming that the hexameric aggregates of H_2DEH[EDP] behave as reverse micelles in solution, cations could be transferred into the hydrophilic cavity of the aggregate without disrupting aggregation while retaining most of their hydration sphere. This view is consistent with the strong water absorption bands observed in the infrared measurements for H_2DEH[EDP].

Based on this extraction mechanism, it was possible to calculate the value of the aggregation constant for H_2DEH[EDP] from the alkaline earth extractant dependency data (17), following an approach similar to that used previously to explain analogous effects in metal ion extraction by dialkylnaphthalene sulfonic acids (30,32). Following this procedure, a β_6 value of $(6 \pm 1)\ 10^{13}$ was obtained.

The aggregation constants for H_2DEH[BuDP] were obtained from osmometric measurements (18). The VPO data for H_2DEH[BuDP] reported in Figure 3 show a small deviation from linearity. The straight line fit of the data has a slope consistent with an average aggregation number of about 3.3. This strongly suggests the formation of predominantly trimeric aggregates in equilibrium with other somewhat larger species. By best fitting the data with mass balance and aggregation equilibria expressions, it was found that the aggregation of H_2DEH[BuDP] in toluene is best described as an equilibrium involving the formation of trimeric and hexameric species with $\beta_3 = (6.2 \pm 1.6)\ 10^6$ and $\beta_6 = (1.8 \pm 0.5)\ 10^{14}$. Using these β values, it is easy to show that the trimer is the predominant H_2DEH[BuDP] species present in solution at concentrations up to 0.1 M. This aggregate is assumed to be the primary metal extracting species.

Figure 1 clearly shows that the solvent extraction behavior of H_2DEH[BuDP] is different from that of H_2DEH[EDP]. It is interesting to note that the H_2DEH[BuDP] trimer and the H_2DEH[EDP] hexamer both contain 12 carbon atoms in the alkyl chain separating the phosphorus atoms. The two aggregates, however, should be different. The internal core of the H_2DEH[BuDP] aggregate should be considerably less hydrophilic than the interior of the H_2DEH[EDP] hexamer because of the smaller number of polar P(O)(OH) groups. As a result, the solvent extraction of metal ions by a H_2DEH[BuDP] trimer is expected to be quite different from that of the H_2DEH[EDP] hexamer.

In the case of the H_2DEH[MDP] dimer, it was not possible to calculate the dimerization constant. The linearity of the VPO data shown in Figure 3 indicates that the dimerization constant is sufficiently large so that the ligand is dimeric over the entire concentration range investigated.

Conformation of the H_2DEH[MDP] dimer

Possible structures for the H_2DEH[MDP] dimer are shown in **III-VI** below:

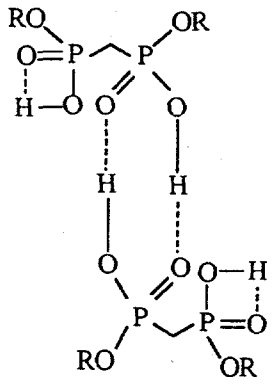

III

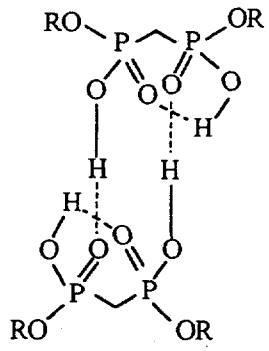

IV

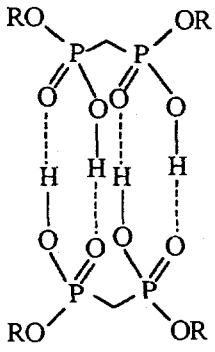

V

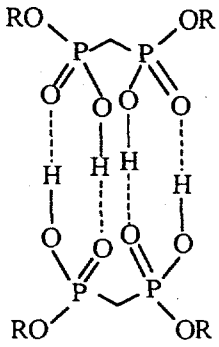

VI

As mentioned earlier, the appearance of two bands in the phosphoryl stretching region of the infrared spectrum of H_2DEH[MDP] suggests that the dimer might contain two different types of hydrogen bonds, as shown in **III** or **IV** (the symmetrical conformatons V and VI only contain intermolecular hydrogen bonds). This possibility was tested by continuous variation infrared spectroscopic studies. In this investigations, the effect on the P=O stretching vibration of progressively replacing the CCl_4 diluent in a solution of H_2DEH[MDP] with the depolymerizing diluent 1-decanol was observed (23). (Note that the spectra of the diphosphonic acids in CCl_4 and toluene are identical, so that the following considerations apply to both diluents (23)).

The intramolecular hydrogen bonds in the $\mathbf{R_1^1(4)}$ and $\mathbf{R_1^1(6)}$ moieties of structure **III** and **IV** are expected to be disrupted by added decanol sooner than the intermolecular hydrogen bonded rings. Thus, the band corresponding to the $\mathbf{R_1^1(4)}$ or $\mathbf{R_1^1(6)}$ moieties should shift gradually as decanol is added. In dimer structures **V** and **VI**, which contain

two adjacent $\mathbf{R_2^2(8)}$ moieties, the entire structure would be destabilized by replacement of any one of the four hydrogen bonds by hydrogen bonds to decanol. The single P=O stretching band anticipated for these structures would be expected to abruptly shift at the decanol concentration at which the dimer dissociates.

The observed infrared spectra of H_2DEH[MDP] in the presence of increasing concentrations of decanol showed that one absorption in the P=O stretching region (1189 cm^{-1}) remained constant even when the CCl_4 solvent was entirely replaced by decanol. The other absorption band in this region remained constant at 1238 cm^{-1} as the solvent was changed incrementally from CCl_4 to a CCl_4-decanol mixture where the decanol concentration was eight times the concentration of the diphosphonic acid. Upon complete replacement of the solvent by decanol, this band shifted abruptly to 1231 cm^{-1}.

Since the 1189 cm^{-1} band is solvent independent and still present when the diphosphonic acids are monomeric, it cannot be reasonably assigned to a hydrogen bonded P=O stretching mode. This band must arise from another mode that coincidentally occurs in this region (23). The 1238 cm^{-1} band of H_2DEH[MDP], therefore, is assigned as the only P=O stretching vibration. The abrupt shift of this band upon complete solvent replacement is consistent with structures **V** and **VI**.

To fully elucidate the relative stability of structures **III-VI**, molecular mechanics calculations were performed. A variety of starting structures containing two (such as **III** and **IV**) or four (such as structures **V** and **VI**) intermolecular hydrogen bonds were generated and geometry-optimized. For ease of computation, the 2-ethylhexyl groups in H_2DEH[MDP] were replaced by methyl groups. Two highly hydrogen bonded dimer structures were found to be the most stable. They exhibited the hydrogen bonding patterns of structures **V** or **VI**. The lowest energy conformation found for structure **VI** was slightly higher in energy than the lowest energy conformation found for structure **V**. The hydrogen bonding in **VI** is expected to be slightly weaker than in **V**, due to larger intermolecular H···H repulsions, as illustrated below.

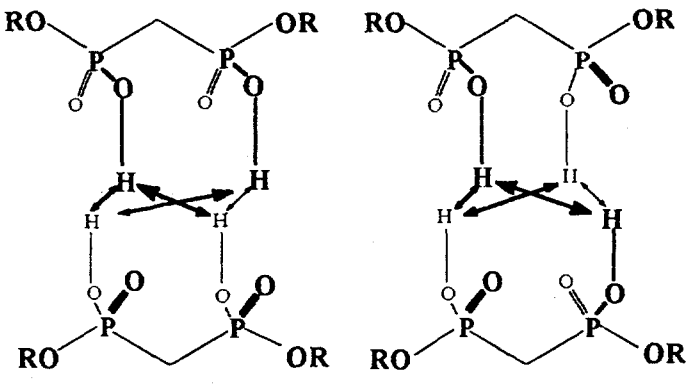

V **VI**

In these structures, the intermolecular proton-proton repulsions in dimer structures **V** and **VI** are represented as arrows. Repulsions are both within $\mathbf{R_2^2(8)}$ rings and between adjacent rings. In structure **V**, the intermolecular inter-ring repulsions are between protons at opposite corners of the dimer; in structure **VI**, they are between protons at adjacent corners. The calculated energy difference is less than 1 kcal mol^{-1}, which suggests that both **V** and **VI** are populated in an equilibrium mixture (23).

SANS investigations

Small Angle Neutron Scattering (SANS) is a powerful technique in structural studies of polymers and micelles (33). Recent studies have shown the applicability of the SANS technique to solvent extraction chemistry. SANS has the unique ability to elucidate the size and shape of both the extractant aggregates and the polymeric species formed upon metal ions extraction (34-37). The need exists for a better knowledge of the species that are formed under conditions likely to be met in practical applications of solvent extractions, i.e., at high metal loading of the organic phase. Under these conditions, large aggregates or polymeric species are often formed that have not been studied in detail (31). The application of SANS to this aspect of solvent extraction chemistry is particularly promising.

SANS studies of the aggregation of H_2DEH[MDP], H_2DEH[EDP] and H_2DEH[BuDP] dissolved in deuterated toluene have been performed (24-26). The results of these studies are summarized in Table 1.

Table 1. Radius of Gyration, $\mathbf{R_g}$, and Aggregation Number, **n**, for Di(2-Ethylhexyl)-Substituted Diphosphonic Acids in Deuterated Toluene

Acid	Molarity	R_g (Å)	n
H_2DEH[MDP]	0.10 M	6.9±0.5	2.1±0.1
H_2DEH[EDP]	0.05 M	10.1±0.5	5.7±0.5
"	0.10 M	10.6±0.6	5.8±0.5
H_2DEH[BuDP]	0.05 M	7.4±1.3	2.9±0.2
"	0.10 M	12.4±0.3	3.6±0.3

The results in Table 1 substantiate the VPO results discussed earlier. The radius of gyration, $\mathbf{R_g}$, of the aggregates is a measure of the spatial extension of the particle. $\mathbf{R_g}$ is given by the root-mean-squared distance of all the atoms from the centroid of the scattering particle. The $\mathbf{R_g}$ values in Table 1 clearly indicate that the H_2DEH[EDP] and H_2DEH[BuDP] aggregates are significantly larger than the H_2DEH[MDP] aggregate.

More specifically, the **n** values of the table confirm that H_2DEH[MDP] exists in solution as a dimer, H_2DEH[EDP] as a hexamer, and H_2DEH[BuDP] predominantly as a trimer. The **n** value obtained for a 0.05 M solution of H_2DEH[BuDP] is slightly lower than that obtained for a 0.1 M solution. This result is consistent with our earlier observations which suggested a low concentration of hexameric aggregates in equilibrium with a higher concentration of H_2DEH[BuDP] trimers (18).

In our attempts to obtain more detailed information about the three-dimensional shape of the H_2DEH[EDP] aggregate, we were able to fit the SANS data with a spherical model with a radius **R** of 11.8 ± 0.2 Å. The fit is shown in Figure 4. In this aggregate, the alkyl groups are likely oriented outwards (toward the solvent) and a large hydrophilic internal cavity is available to accomodate metal cations and/or water molecules.

Because the VPO data discussed earlier revealed the tendency of some metal-extractant complexes to aggregate extensively in the organic phase, SANS measurements were also performed on deuterated toluene solutions of the three diphosphonic acids after extraction of progressively higher concentrations of selected metal cations (24-26).

Both U(VI) and Th(IV) form large aggregates with H_2DEH[MDP]. This is particularly true for Th(IV) for which aggregates containing up to ~200 ligand molecules were identified (25). These aggregates grow in three dimensions and it is likely that that these species have the same three-dimensional structure as the Th(DEH[MDP])$_2$ salt that precipitates under very high metal loading conditions in the biphasic system used to extract Th(IV).

The Fe(III)-H_2DEH[MDP] system is particularly striking. The SANS results confirm the tendency of the Fe(III) complexes with H_2DEH[MDP] to aggregate extensively. Further, the measurements reveal the presence of rod-like particles of constant radius but variable length which depends on the concentration of metal in the organic phase. As more metal is brought into the organic phase, particle growth is propagated by attachment to terminal sites of the existing rod-like aggregates. Table 2 reports the radius of gyration, aggregation number, and radius and length of the rod-like particles identified after extraction of Fe(III) from aqueous solutions containing different HNO_3 concentrations.

The average radius of 9 Å for the aggregates reported in Table 2 agrees with results of previous SANS investigations on monofunctional analogues of H_2DEH[MDP] (34). It is reasonable to assume that the hydrocarbon chains of the ester are oriented toward the exterior of the cylindrical aggregates, while the metal ions interact with the polar groups of the extractant which are oriented toward the interior of the cylinder. The metal ions thus are located along a channel in the center of the cylinder. If this is the case, a plausible structure of the metal-extractant polymeric species is shown in Structure **VII**. Similar structures have been recently observed for solid-state, eight- and seven-coordinate, crystalline lanthanide complexes of 1-hydroxyethane-1,1-diphosphonic acid, HEDPA (an aqueous soluble, non-alkyl-substituted analogue of H_2DEH[MDP] (38).

Table 2. Gyration Radius (R_g), Aggregation Number (**n**), Radius (**R**) and Length (**L**) for Rod-Shaped Aggregates formed in the extraction of Fe(III) by 0.1 M H_2DEH[MDP].

$[Fe]_{org}$ M	$[H_2DEH[MDP]]/[Fe]_{org}$	R_g, Å	n	R, Å	L, Å
0.00972[a]	10.29	7.4 ± 0.3	2.8 ± 0.04	/	/
0.0252[a]	3.96	8.3 ± 0.3	4.6 ± 0.05	/	/
0.0447[a]	2.24	20 ± 0.7	17 ± 0.2	8.8 ± 0.4	66
0.0586[a]	1.71	70 ± 7.9	70 ± 4	10.2 ± 0.5	241
0.0248[b]	4.03	8.4 ± 0.4	4.2 ± 0.07	/	/
0.0413[b]	2.42	17 ± 1.1	12 ± 0.3	8.9 ± 0.6	55
0.0540[b]	1.85	30 ± 1.8	21 ± 2	8.9 ± 0.6	102
0.0589[b]	1.70	88 ± 30	110± 22	7.6 ± 0.1	304
0.0240[c]	4.17	7.7 ± 0.4	4.1 ± 0.07	/	/
0.0463[c]	2.16	35 ± 3.3	23 ± 0.8	8.9 ± 0.4	119
0.0551[c]	1.81	48 ± 3.7	36 ± 4	8.9 ± 0.5	165
0.0476[c]	2.18	80 ± 7.9	69± 5	10.2 ± 0.2	276

a. Fe(III) extracted from 0.1 M HNO_3.
b. Fe(III) extracted from 1 M HNO_3.
c. Fe(III) extracted from 5 M HNO_3.

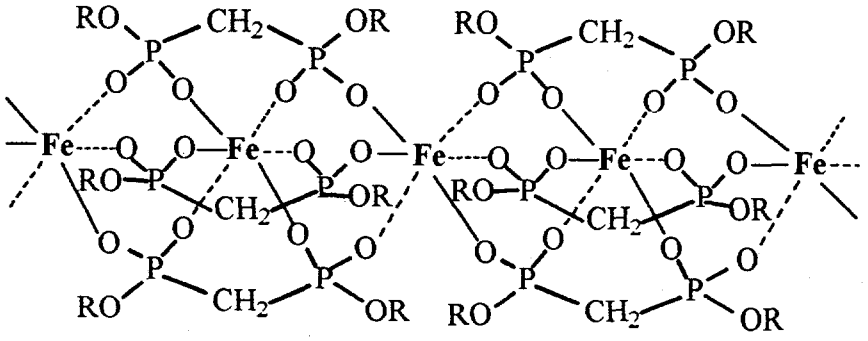

Structure **VII**

Assuming a structure of this type for the Fe(III)-H_2DEH[MDP] aggregates, the SANS data have been used to calculate the distance between neighboring Fe(III) atoms in the chain (24). The Fe-Fe distance in the Fe(III)-H_2DEH[MDP] aggregates was calculated to be 3.7 ± 0.3 Å. This value is reasonable in view of the 4.7 to 5.8 Å metal-metal distances found in lanthanide HEDPA complexes (41). Structure **VII** and the 3.7 Å value of the Fe-Fe distance suggest formation of covalent bonds between Fe(III) and the ligand

molecules. Covalent binding of Fe(III) to H_2DEH[MDP] has been experimentally confirmed in a far-infrared investigation of the Fe(III)-H_2DEH[MDP] complex (21).

Surprisingly, the SANS data did not indicate formation of large aggregates for the extraction of Fe(III) by H_2DEH[EDP]. The highest aggregation number for the Fe(III)-H_2DEH[EDP] complex was ~8. Apparently, the increase in the length of the alkyl bridge connecting the two P atoms of the ligand by one CH_2 group, not only has a profound effect on the state of aggregation of the extractant itself, but also on the tendency of metal complexes to extensively aggregate.

The **n** values measured for H_2DEH[EDP] solutions after extraction of Ca(II), La(III), and U(VI) are not significantly different from that of the extractant alone. In these cases the aggregation number is ~6. It was mentioned earlier that the extraction of some cations does not alter the infrared spectrum of the extractant and that water is co-extracted. Thus, the SANS results confirm that metal extraction occurs primarily through cation transfer into the hydrophilic cavity of the hexameric aggregate with little, if any, disruption of the solution structure of the extractant. This type of extraction, reminiscent of metal extraction by reverse micelles, is consistent with the the extractant dependencies measured for alkaline earth cations, Am(III), and U(VI) (see, for example, Figure 1). The SANS data obtained for a U(VI)-H_2DEH[EDP] solution with a ligand to metal ratio of ~2 were fitted with a spherical particle model with a radius of 12.4 ± 0.5 Å. If the reverse micelle analogy applies to this solution, the **n** value of ~6 implies that three uranyl ions are present in the internal cavity of the hexameric aggregate. Thus, the spherical hexameric aggregate of H_2DEH[EDP] does not change its structure even at the maximum U(VI) loading attainable.

Large aggregates were also identified in solutions containing Fe(III)-H_2DEH[BuDP] complexes (26). As with the Fe(III)-H_2DEH[MDP] particles, these aggregates are rod-shaped. There is, however, a difference between the two systems. The Fe(III)-H_2DEH[MDP] aggregates have a constant radius and grow lengthwise with increasing Fe(III) concentration (24). In contrast, the Fe(III)-H_2DEH[BuDP] aggregates have an approximately constant length and a radius that increases with the Fe(III) concentration in the organic phase. It is likely that growth of the rod-like Fe(III)-H_2DEH[BuDP] aggregates occurs along the axis of the rod as shown in Structure **VIII**:

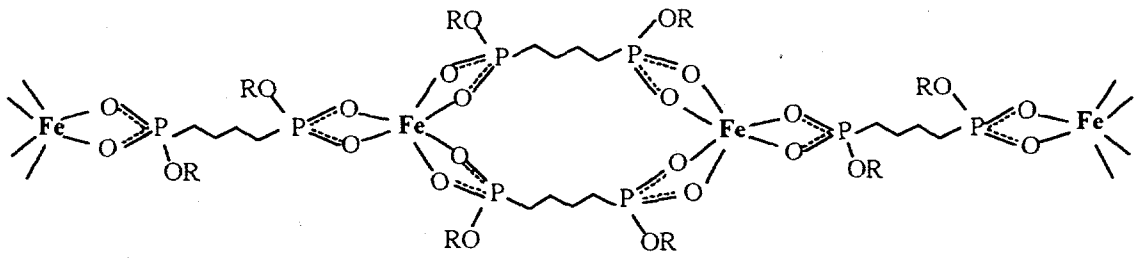

Structure **VIII**

In these aggregates, each Fe(III) atom only interacts with phosphonate groups belonging to different ligand molecules. In H_2DEH[BuDP], the donor atoms of the ligand are too far apart to interact simultaneously with the same metal atom. Solvent extraction studies have shown that H_2DEH[BuDP] interacts with metal ions in a way that is similar to its monofunctional analogues. The phosphonate groups of the ligand act independently from one another and complex metal ions in a non-cooperative manner (18). With increasing metal concentration, the rod-like particles initially formed grow thicker. This growth presumably occurs via opening of the ring formed by two ligand molecules bound to adjacent Fe(III) atoms. In this way, two sidearms form that grow independently in a three-dimensional network.

CONCLUSIONS

The aggregation of the solvent extraction reagents P,P'-di(2-ethylhexyl) methane-, ethane- and butanediphosphonic acids (H_2DEH[MDP], H_2DEH[EDP] and H_2DEH[BuDP], respectively) in toluene solutions has been investigated using the complementary techniques of infrared spectroscopy, vapor pressure osmometry (VPO), molecular mechanics and small angle neutron scattering (SANS).

The results of our investigations have shown that the length of the alkyl chain separating the two P atoms of the extractant molecule has a profound effect on the aggregation state of the extractant. The extractant's aggregation state, in turn, strongly affects the metal solvent extraction chemistry.

Experimental and computational evidence established that H_2DEH[MDP] is a dimer in toluene. The aggregate is stabilized by strong hydrogen bonding. The most stable conformation of the dimer is a closed, symmetrical structure containing only intermolecular hydrogen bonds with two adjacent $\mathbf{R_2^2(8)}$ rings and a larger $\mathbf{R_2^2(12)}$ moiety, such as structures **V** and **VI**.

H_2DEH[EDP] forms hexameric, spherical aggregates in toluene. The hexameric H_2DEH[EDP] aggregates most likely adopt a structure comparable to that of reverse micelles. In these aggregates, the alkyl groups are oriented toward the solvent and a large hydrophilic internal cavity is available to accomadate metal cations. The highly aggregated state of H_2DEH[EDP] and the fact that the aggregation is not disrupted by the extraction of several metal cations has been used to explain the extractant dependencies of unity measured for the extraction of alkaline earth cations, Am(III) and U(VI). These metal ions are transferred into the hydrophilic cavity of the aggregate without disrupting its structure while retaining most or part of their hydration sphere.

The aggregation of H_2DEH[BuDP] in toluene is best described as an equilibrium involving the formation of trimeric and hexameric species. The trimer is the predominat species in the concentration range investigated. The internal core of the H_2DEH[BuDP] aggregate is less hydrophilic than that of the H_2DEH[EDP] hexamer because of the

smaller number of polar P(O)(OH) groups. Consequently, the H_2DEH[BuDP] aggregates do not behave as reverse micelles in metal solvent extraction.

SANS investigations have demonstrated that large aggregates form when solutions of H_2DEH[MDP] and H_2DEH[BuDP] are used to extract certain metal ions under high metal loading conditions. The largest aggregates observed were in the extraction of Fe(III) and Th(IV). The Fe(III)-H_2DEH[MDP] aggregates are rods of constant radius whose length increases with the metal concentration in the organic phase. The Th(IV)-H_2DEH[MDP] and Fe(III)-H_2DEH[BuDP] aggregates are cylindrical but growth also occurs laterally as more metal is transferred into the organic phase.

The formation of large aggregates has important implications for practical application of solvent extraction reagents. For example, if the extraction chromatographic resin Dipex, which contains H_2DEH[MDP] adsorbed in the pores of an inert support (4), is used to separate metal ions such as Fe(III) and actinides from solutions where the metal concentrations are relatively high, aggregated species may form. Because of their higher viscosity, these species might slow down or even prevent further metal uptake. Stripping of the sorbed metal species from the resin, under these conditions, could also become difficult. Similar complications could arise in more conventional liquid-liquid solvent extraction procedures due to the formation of polymeric interfacial cruds even at relatively low metal loading of the organic phase.

ACKNOWLEDGMENTS

The work performed at ANL was funded by the U.S. Department of Energy, Office of Basic Energy Science, Division of Chemical Science, under contract W-31-109-ENG-38.

We wish to thank Ken Nash (ANL Chemistry Division) and Phil Horwitz (PG Research Foundation, Inc., Darien, IL) for useful discussion and advice, and Volker Urban and Pappanan Thiyagarajan (ANL, IPNS) for introducing the authors to the small angle neutron scattering technique.

REFERENCES

1. E.N.Rizkalla, Rev. Inorg. Chem., *5*, 223 (1983).
2. K.L.Nash, Radiochimica Acta, *54*, 178 (1991).
3. R.Chiarizia, E.P.Horwitz, S.D.Alexandratos and M.J.Gula, Sep. Sci. Technol., *32*, 1 (1997), *and references therein.*
4. E.P.Horwitz, R.Chiarizia and M.L.Dietz, Reactive and Functional Polymers, *33*, 25 (1997) and US Patent 5,651,883, issued on July 29, 1997.
5. Y.Marcus and A.S.Kertes, *Ion Exchange and Solvent Extraction of Metal Complexes*, John Wiley & Sons Ltd., New York, NY, 1969.
6. Z. Kolarik, Solvent Extr. Reviews, *1*, 1 (1971).
7. M.C.Etter, Acc. Chem. Res., *23*, 120 (1990).
8. D.F.Peppard, J.R.Ferraro, and G.W.Mason, J. Inorg. Nucl. Chem., *12*, 60 (1959).
9. D.F.Peppard, J.R.Ferraro, and G.W.Mason, J. Inorg. Nucl. Chem., *7*, 231 (1958).
10. D.F.Peppard, G.W.Mason, W.J.Driscoll and R.J.Sironen, J. Inorg. Nucl. Chem., *7*, 276 (1958).
11. J.R.Ferraro, G.W.Mason and D.F.Peppard, J. Inorg. Nucl. Chem., *22*, 285 (1961).
12. G.S.Rao, G.W.Mason and D.F.Peppard, J. Inorg. Nucl. Chem., *28*, 887 (1966).
13. G.W.Mason, S.McCarty and D.F.Peppard, J. Inorg. Nucl. Chem., *24*, 967 (1962).
14. R.Chiarizia, R.C.Gatrone and E.P.Horwitz, Solv. Extr. Ion Exch., *13*, 65 (1995).
15. E. Högfeldt, R.Chiarizia, P.R.Danesi and V.S.Soldatov, Chemica Scripta, *18*, 13 (1981).
16. R.Chiarizia, E.P.Horwitz, P.G.Rickert and A.W.Herlinger, Solvent Extr. Ion Exch., *14*, 773 (1996).
17. R.Chiarizia, A.W.Herlinger and E.P.Horwitz, Solvent Extr. Ion Exch., *15*, 417 (1997).
18. R.Chiarizia, A.W.Herlinger, Y.D.Cheng, J.R.Ferraro, P.G.Rickert and E.P.Horwitz, Solvent Extr. Ion Exch., *16*, 505 (1998).
19. A.W.Herlinger, R.Chiarizia, J.R.Ferraro, and E.P.Horwitz, Polyhedron, *16*, 1843 (1997).
20. A.W.Herlinger, R.Chiarizia, J.R.Ferraro, P.G.Rickert and E.P.Horwitz, Solvent Extr. Ion Exch., *15*, 401 (1997).
21. A.W.Herlinger, J.R.Ferraro, J.A.Garcia and R.Chiarizia, Polyhedron, *17*, 1471 (1998).
22. J.R.Ferraro, A.W.Herlinger and R.Chiarizia, Solvent Extr. Ion Exch., *16*, 775 (1998).
23. R.E.Barrans Jr., D.R.McAlister, A.W.Herlinger, R.Chiarizia and J.R.Ferraro, Solvent Extr. Ion Exch., *17*, 1195 (1999).
24. R.Chiarizia, V.Urban, P.Thiyagarajan and A.W.Herlinger, Solvent Extr. Ion Exch., *16*, 1257 (1998).
25. R.Chiarizia, V.Urban, P.Thiyagarajan and A.W.Herlinger, Solvent Extr. Ion Exch., *17*, 113 (1999).
26. R.Chiarizia, V.Urban, P.Thiyagarajan and A.W.Herlinger, Solvent Extr. Ion Exch., *17*, 1133 (1999).
27. J.R.Ferraro, D.F.Peppard and G.W.Mason, J. Inorg. Nucl. Chem., *27*, 2055 (1965).

28. L.C.Thomas, *Interpretation of the Infrared Spectra of Organophosphorus Compounds*, Heyden, London, UK, 1974.
29. K.Moedritzer and R.R.Irani, J. Inorg. Nucl. Chem., *22*, 297 (1961).
30. B.A.Moyer, C.F.Baes, Jr., G.N.Case, G.J.Lumetta and N.M.Wilson, Sep. Sci. Technol., *28*, 81 (1993).
31. R.D. Neuman, N.F. Zhou, J. Wu, M.A. Jones, A.G. Gaonkar, S.J. Park and M.L. Agrawal, Sep. Sci. Technol., *25*, 1655 (1990).
32. R. Chiarizia, P. R. Danesi, M. A. Raieh and G. Scibona, J. Inorg. Nucl. Chem., *37*, 1495 (1975).
33. L.J.Magid, *Structure and Dynamics by Small-Angle Neutron Scattering*, in *Nonionic Surfactants, Physical Chemistry*, M.J.Schick Ed., Surfactant Science Series, vol. 23, Marcel Dekker, Inc., New York, 1987.
34. P.Thiyagarajan, H.Diamond, P.R.Danesi and E.P.Horwitz, Inorg. Chem., *26*, 4209 (1987).
35. P.Thiyagarajan, H.Diamond and E.P.Horwitz, J. Appl. Cryst., *21*, 848 (1988).
36. H.Diamond, P.Thiyagarajan and E.P.Horwitz, Solv. Extr. Ion Exch., *8*, 503 (1990).
37. D.C.Steytler, T.R.Jenta, B.H.Robinson, J.Eastoe and R.K.Heenan, Langmuir, *12*, 1483 (1996).
38. K.L.Nash, R.D.Rogers, J.R.Ferraro and J.Zhang, Inorg. Chim. Acta, *269*, 211 (1998).

Figure Captions

Figure 1. Distribution ratio, **D**, vs initial extractant concentration in the extraction of Am(III) by H_2DEH[MDP], H_2DEH[EDP] and H_2DEH[BuDP] in o-xylene from aqueous solutions containing different concentrations of HNO_3.

Figure 2. Infrared spectra of 0.15 M toluene solutions of H_2DEH[MDP] (a), H_2DEH[EDP] (b), and H_2DEH[BuDP] (c).

Figure 3. Osmometric measurements with H_2DEH[MDP], H_2DEH[EDP] and H_2DEH[BuDP] in toluene at T = 25 °C. Standard = bibenzyl. Slope values of the lines and aggregation numbers (**n**) are shown in the figure.

Figure 4. Fit of the SANS data for 0.1 M H_2DEH[EDP] in deuterated toluene with a spherical particle model. **I(Q)** is the scattering intensity and **Q** is the momentum transfer, defined as $(4\pi/\lambda)\sin\theta$, where θ is half the scattering angle and λ is the wavelength of the neutrons.

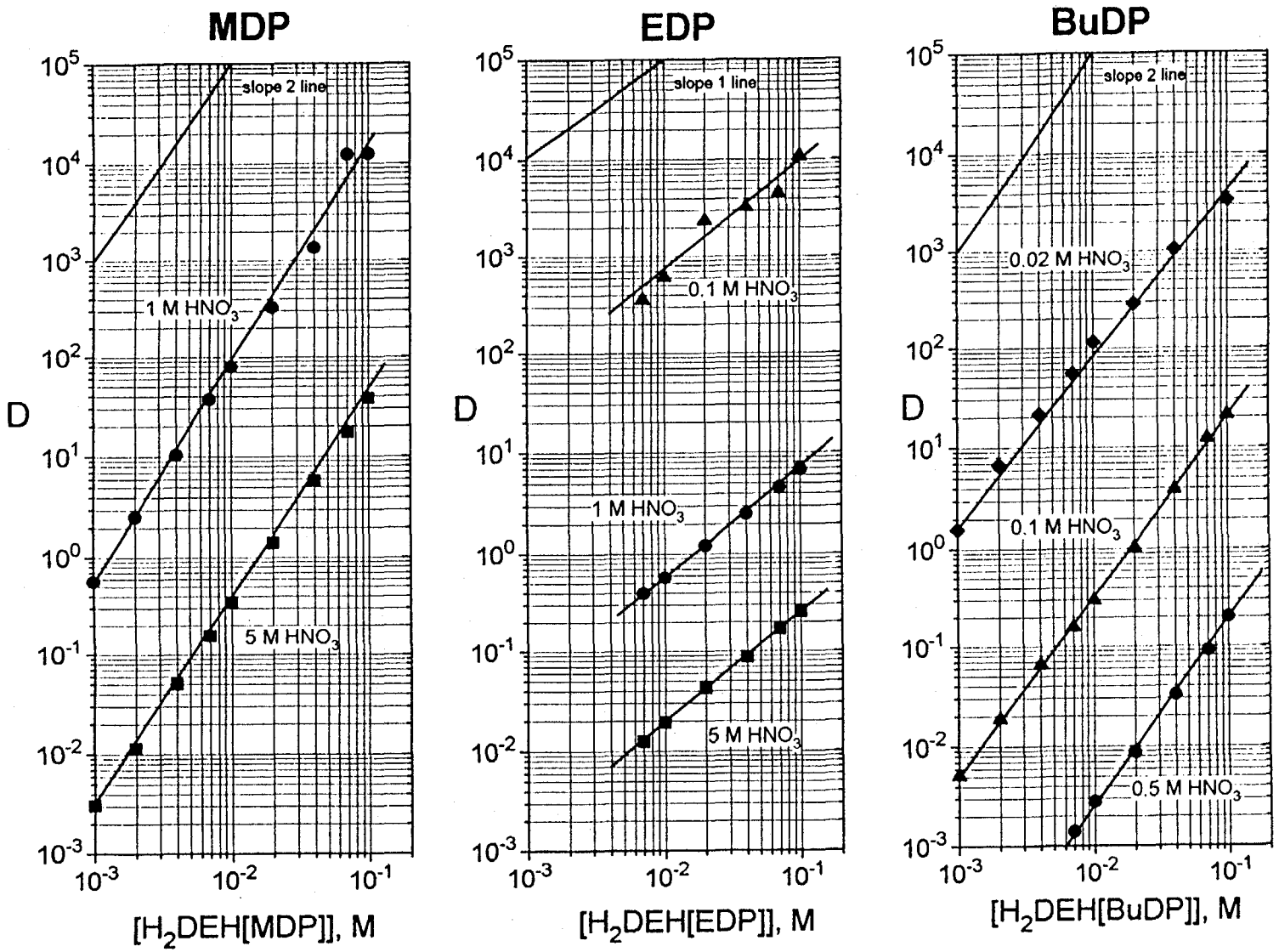
MDP
slope 2 line
1 M HNO3
5 M HNO3
D
[H2DEH[MDP]], M
EDP
slope 1 line
0.1 M HNO3
1 M HNO3
5 M HNO3
D
[H2DEH[EDP]], M
BuDP
slope 2 line
0.02 M HNO3
0.1 M HNO3
0.5 M HNO3
D
[H2DEH[BuDP]], M

Figure 1

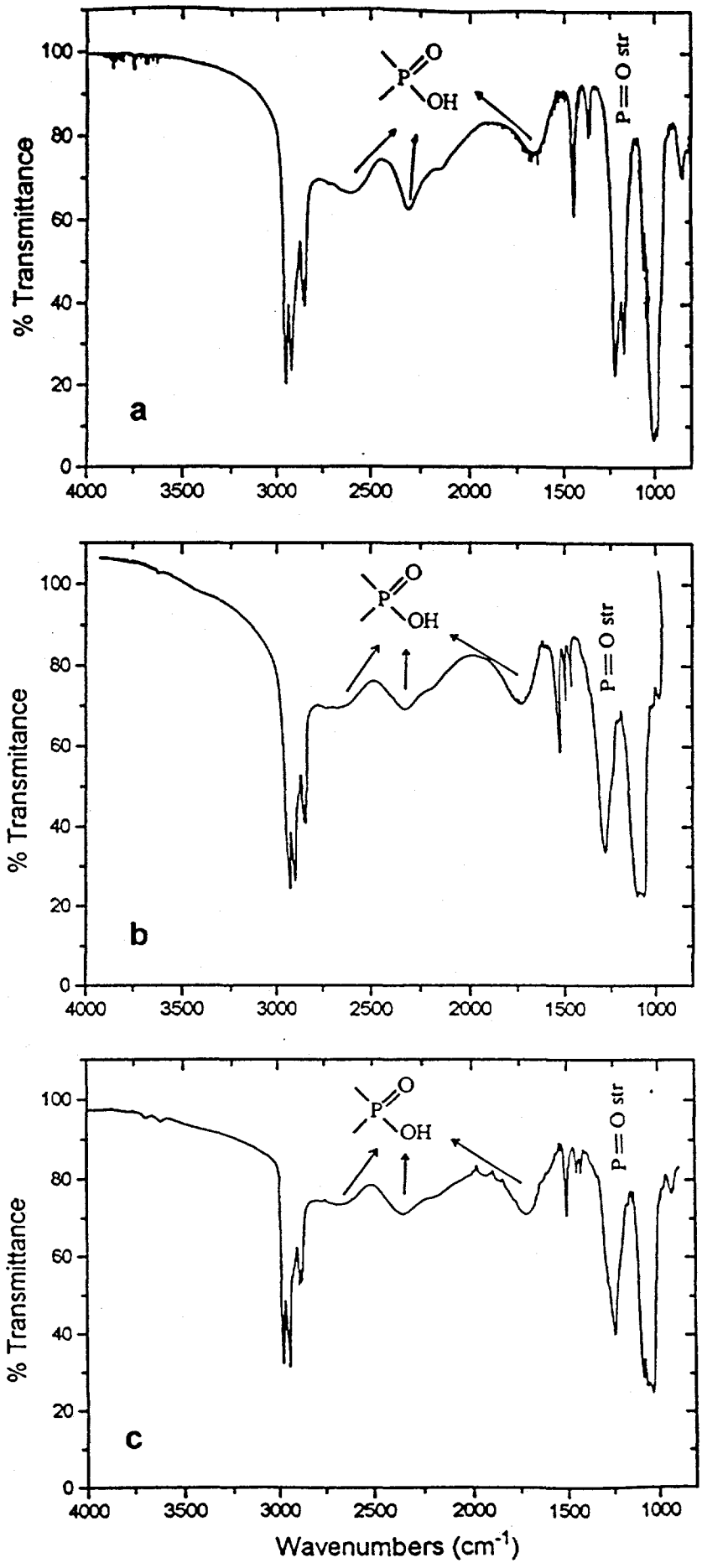
% Transmittance
100
80
60
40
20
0
4000
3500
3000
2500
2000
1500
1000
P=O
OH
P=O str
a
% Transmitance
b
% Transmittance
c
Wavenumbers (cm-1)

Figure 2

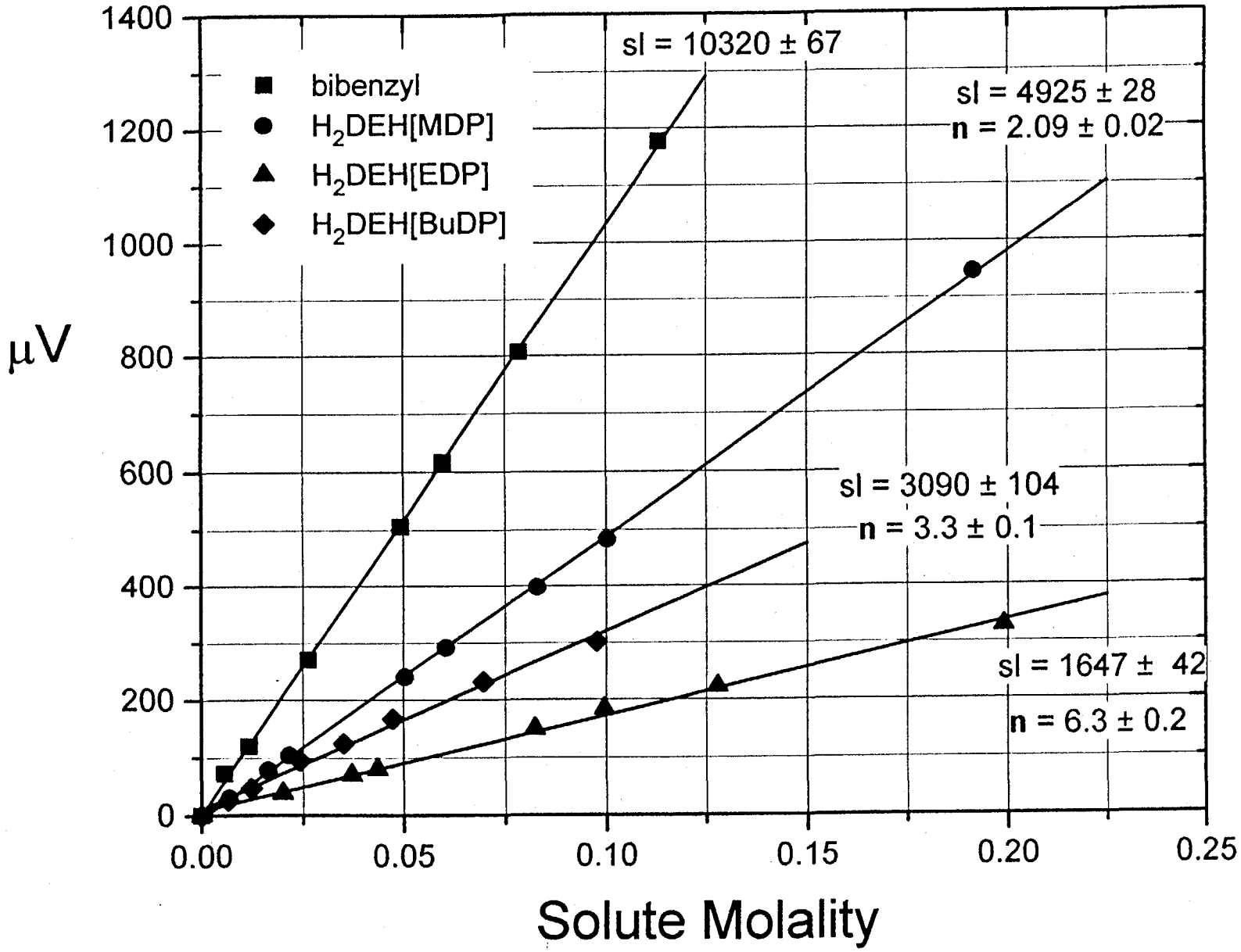
1400
1200
1000
800
600
400
200
0
μV
0.00
0.05
0.10
0.15
0.20
0.25
Solute Molality
bibenzyl
H2DEH[MDP]
H2DEH[EDP]
H2DEH[BuDP]
sl = 10320 ± 67
sl = 4925 ± 28
n = 2.09 ± 0.02
sl = 3090 ± 104
n = 3.3 ± 0.1
sl = 1647 ± 42
n = 6.3 ± 0.2

Figure 3

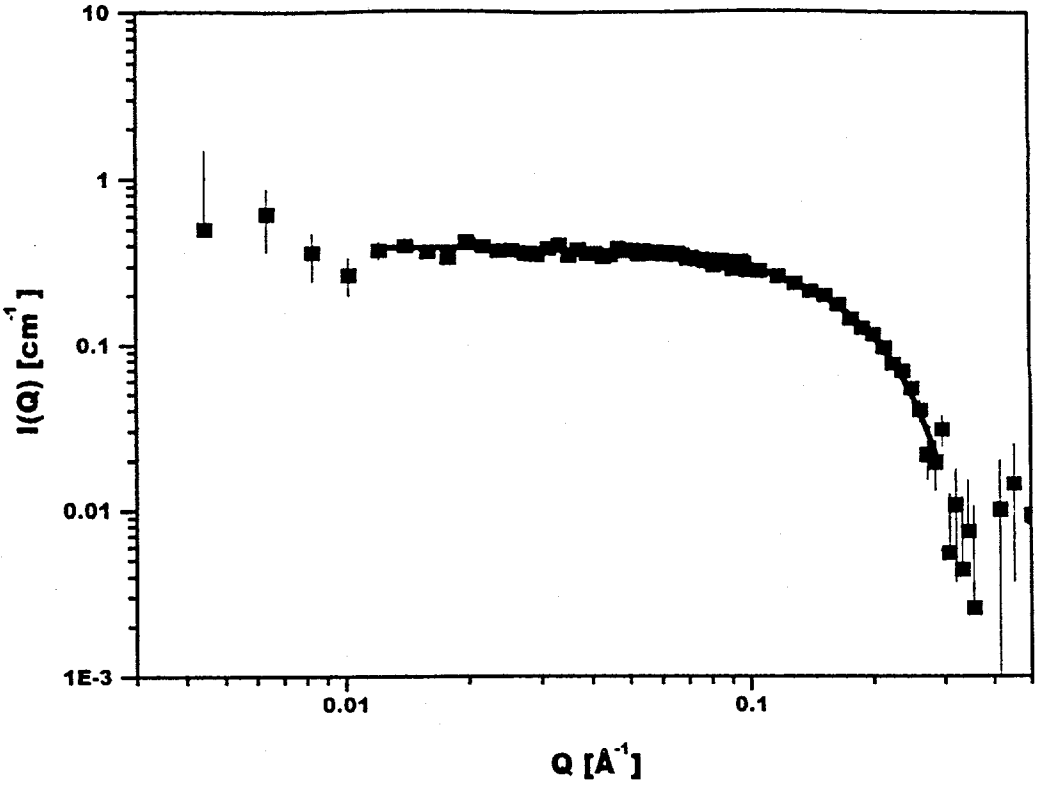

Figure 4